NASA TECHNICAL NOTE

NASA TN D-3328

SIMULATED NUCLEAR HEATING OF LIQUID HYDROGEN IN A PROPELLANT TANK

by Sidney C. Huntley and James W. Gauntner

Lewis Research Center
Cleveland, Ohio

NATIONAL AERONAUTICS AND SPACE ADMINISTRATION • WASHINGTON, D. C. • MARCH 1966

SIMULATED NUCLEAR HEATING OF LIQUID HYDROGEN IN A PROPELLANT TANK

By Sidney C. Huntley and James W. Gauntner

Lewis Research Center
Cleveland, Ohio

NATIONAL AERONAUTICS AND SPACE ADMINISTRATION

For sale by the Clearinghouse for Federal Scientific and Technical Information
Springfield, Virginia 22151 – Price $2.00

SIMULATED NUCLEAR HEATING OF LIQUID HYDROGEN IN A PROPELLANT TANK

by Sidney C. Huntley and James W. Gauntner

Lewis Research Center

SUMMARY

An experimental study was made to simulate nuclear heating of liquid hydrogen in a propellant tank by using an electrical immersion heater and radiant heaters. Flow tests were made in a 125-gallon tank pressurized to 2 atmospheres with a flow rate of about 0.04 pound per second. Test results showed that the inoperative immersion heater did not alter the exit temperature history. Operation of the immersion heater tended to result in a more completely mixed liquid than existed with nuclear heating. A comparison of bottom (radiant) heating with nuclear heating showed a nearly identical generalized exit temperature history with a similar generalized heat input rate distribution and equal heating parameters, although the initial total heat input rates varied by a factor greater than 6. High bottom (or liquid source) heating was observed to consistently result in a liquid disturbance near the surface during the transient development of a temperature gradient.

INTRODUCTION

Interest in propellant heating has increased in recent years because of the desire to achieve minimum rocket vehicle weight. A knowledge of the effects of propellant heating on such vehicle components as the propellant tank, the pressurization system, and the pump is desirable for optimization of the vehicle weight. Propellant heating in most rocket vehicles consists of a net influx of heat to the propellant from thermal radiation and aerodynamic heating of the tank walls. Additional heating of the propellant in a nuclear vehicle results from nuclear radiation absorbed both in the tank walls and in the propellant itself. The propellant heating problem arises from uncertainties regarding the liquid behavior when subjected to one or more of the aforementioned heat loads. A knowledge of the liquid behavior is required in making a compromise between tank pressure level necessary to provide the net positive suction head requirements of the pump and the extent of thermal protection from the external heating loads.

In the early phases of the nuclear rocket program there was little information describing the effect of wall and nuclear (or source) heating on liquid behavior. One of the first analytical studies of the problem, appearing in reference 1, consisted of a numerical approach to predict transient temperature

profiles in the fluid either for closed tanks or for tanks with flow. There were no experimental nuclear data available for comparison. A qualitative investigation of noncryogenic liquid behavior in a vented two-dimensional glass tank subjected to wall and source heating was conducted at NASA Lewis Research Center (ref. 2). An extension of this program consisting of an analytical and experimental investigation was made of the effects of nuclear heating on the temperature histories of liquid hydrogen. This investigation was conducted using a three-dimensional tank representing a scaled-down version of a proposed nuclear rocket propellant tank (refs. 3 to 5). Another experimental investigation of side wall and bottom heating of liquid hydrogen contained in a tank similar to that of reference 3 was made and is presented in reference 6. The results of the work reported in references 2 to 6 show that the liquid behavior associated with side wall and nuclear (or bottom) heating tends to form a stratified region of warm fluid above a region of turbulently mixed fluid having a uniform temperature. An analysis was developed (ref. 5) and found to predict satisfactorily temperature histories for cases with a major portion of the heating from below. The stratified region, formed by the accumulation of boundary layer flow up the tank walls, was found to be dependent on the ratio of side wall heat flux to bottom heat flux. Low values of this ratio were found to yield thin stratified regions; high values resulted in the entire liquid height being stratified. The effect of variations in this ratio on the temperature history of the liquid at the tank exit during constant pressure outflow was also shown. In addition, it was shown that the effects of total heating rate, flow rate, and tank pressure on the exit temperature history could be generalized. It was further indicated that similar temperature histories were obtained from bottom heating as from nuclear heating provided that the heat input rate distributions were similar.

The purpose of this report is to present the results obtained in an experimental investigation of electrical simulation of nuclear heating of liquid hydrogen. The electrical simulation utilized an immersion heater to produce heat sources in the liquid from the heating of high-resistance 0.020-inch wire elements arranged in a 1/4-inch-wide by 1-inch-high grid network. Nuclear heating of the tank wall was simulated by using radiant heaters. This work was undertaken because of the complex and inflexible nature of performing tests in a nuclear environment. The nuclear environment of reference 3, the only available source of nuclear heating data with liquid hydrogen, was selected as a specific case for simulation. Simulated nuclear heating tests were performed in the tank described in reference 6. Data were also obtained to determine the effect of the presence of the immersion heater (without power applied). The high bottom (radiant) heating work of reference 6 was extended to more nearly duplicate nuclear heating (without simulated source heating) and these results are also presented. The data are generalized in accordance with a set of scaling rules (presented in ref. 6) to make them comparable with other data obtained at different operating conditions.

APPARATUS

The apparatus used in this investigation, with the exception of the immersion heater, was described in detail in reference 6; consequently, only a brief

description is included herein. The test apparatus consisted of the test tank enclosed in a vacuum chamber with provisions for supplying liquid hydrogen, pressurizing and venting the tank, throttling the outflow of liquid, providing source heating of the liquid with electrical elements, and providing separately controlled heating of the tank wall and bottom (fig. 1). A vacuum system was provided which had the capability of producing a vacuum of less than 10^{-5} torr, thereby reducing the conductive heat leak through the vacuum space to a negligible amount.

Tank with Radiant Heaters

An exterior view of the tank with radiant heaters installed is shown in figure 2. The tank, constructed of 304 stainless steel, had a liquid capacity of about 125 gallons with a diameter of 32 inches. The tank geometry consisted of cylindrical walls with a 45° half-angle conical bottom. Spherical sections were used to join the wall and bottom sections and to provide the bottom section with a small radius. A flange and transition section on top of the cylinder was provided for removal of the tank from the elliptical tank dome. The outer surface of the tank and the inner surfaces of both the wall and bottom heaters were sand blasted and spray painted with a flat black lacquer to provide high emissivity surfaces for radiant heat exchange between the tank and heater surfaces.

The radiant heaters were constructed from 304 stainless steel ribbons. The wall heater consisted of a double lead coil of 1- by 1/16-inch ribbon cylindrically wrapped with a $37\frac{1}{2}$-inch inside diameter and a $2\frac{1}{4}$-inch pitch. Each coil had approximately 13 convolutions. The bottom ends of each coil were joined with a length of the heater material to form one continuous strip to which electrical power leads were attached at each end. The overall height of the wall heater was about 30 inches.

The bottom heater consisted of a double lead coil of 3/4- by 1/16-inch ribbon helically wrapped with a 45° half angle from the axis with a major diameter of $36\frac{3}{4}$ inches using a $1\frac{3}{4}$-inch pitch. Each coil had approximately 13 convolutions with the bottom two lead ends joined to form one continuous strip.

The double lead coils of one continuous strip were used for both the wall and bottom heaters to prevent inductive coupling between the heaters and the tank. Voltage-regulated alternating current was separately supplied to each heater.

Immersion Heater

The immersion heater (fig. 3) consisted of 25 individually controlled electric horizontal heating elements, each one being a continuous piece of 0.020-inch wire, having been wound on a form, stress relieved, and then epoxied to a frame of 1/8-inch stainless steel wire which itself had been previously

stress relieved. A wire having essentially constant resistivity in the temperature range from 36° to 500° R was used. The 25 individual heater elements were assembled with the horizontal wires of each element at 90° with respect to the horizontal wires of the two adjacent elements to deter the development of unnatural flow patterns in the liquid.

A 1/2-inch clearance between the heater assembly and the tank wall was allowed to provide space for boundary layer movement and instrumentation leads. Because nuclear source heating yields a relatively smooth gradient of heating rate, it can be more closely simulated by heat sources whose horizontal and vertical spacings are very small; however, practical considerations of construction led to the use of 1/4-inch horizontal spacing between wires and 1-inch vertical spacing between elements. The nuclear source heating load (heating rate per unit volume) of reference 3 decreased exponentially with height of liquid, and the heating load half way up the tank was only about 10 percent of the heating load at the bottom. Consequently, the heater was only extended about half way ($24\frac{1}{2}$ in.) up from the bottom of the tank.

A constant heating load in the radial direction was assumed to be an adequate simulation of the nuclear heating load experienced in reference 3.

Instrumentation

Two temperature measurement systems were used for the test: one consisted of carbon resistors to measure temperatures in the cryogenic temperature range and the other of copper constantan thermocouples to measure gas temperatures. Thirty carbon-resistor thermometers were mounted on a rake extending down the tank axis. These thermometers, spaced at 1/4-inch intervals near the liquid surface of the full tank and at 4-inch intervals elsewhere, were used to observe cryogenic temperatures. A thermometer placed at the tank exit was used to observe the liquid temperature leaving the tank. Temperature data are presented in this report for thermometers located at 0, 16.9, 24.7, 32.7, and 40.7 inches above the exit port along the tank center axis. Additional data for one test are shown for thermometers spaced at 1/4-inch intervals near the initial liquid surface. Thirty-six copper-constantan thermocouples, mounted along the entire axis of the tank at 4-inch, or less, intervals on the axial rake, were used to observe gas temperatures. Three thermocouples were attached to the inner surface of each radiant heater to measure heater temperature. Previous experience with the carbon resistors gave indication that an accuracy within 0.1° R was obtainable in the range of liquid hydrogen temperatures. The thermocouple accuracy was estimated to be within 1° R at temperature levels greater than 138° R.

Other types of measurements included tank pressure, liquid outflow rate, and liquid level position.

PROCEDURE

The desired temperatures on the radiant heaters were established to obtain both the desired wall heat flux and the desired bottom heat flux into the tank. These temperatures were adjusted by varying the electrical input power to each heater. If the particular test required source heating, power was applied to the immersion heater so as to achieve a specified gradient of source heating rate per unit volume as a function of distance from the bottom of the tank. This gradient was similar to the nuclear heating deposition gradient which was experienced in the nuclear tests (ref. 3). After both sets of heaters were operating, the tank was closed and 5 seconds later the tank was pressurized with hydrogen gas to 1 atmosphere above the initial pressure level. The liquid hydrogen was initially at saturation temperature corresponding to the initial pressure level. Next, the fill valve was closed (fig. 1). After the tank had been closed for 20 seconds and a stable pressure achieved, the shutoff valve (fig. 1) was opened and the outflow of hydrogen began at a rate of about 0.04 pound per second controlled by the throttle valve. Additional pressurizing gas was used as needed to maintain a constant tank pressure during the entire flow run.

Both the double wall of the outer shell and the tub-like enclosure around the shutoff valve (see fig. 1) were filled with liquid nitrogen to ensure a constant reproducible temperature which would yield a low ambient heat leak. Uniformity in the initial conditions was obtained by opening the throttle valve with the tank shutoff valve closed and flowing liquid hydrogen from the supply dewar to chill the venturi and to establish the throttle valve setting to achieve the desired flow rate for approximately 15 minutes prior to start of outflow from the tank.

Test conditions for the several experiments are presented in table I. Each test run is identified by run number, the type of heating applied, and the average values of wall heat flux and bottom heat flux are shown. Also shown are the initial height of liquid, the initial liquid temperature, the tank pressure with resulting saturation temperature rise, and the flow rate. The other items will be discussed later.

DATA ANALYSIS

The heat input rate from the radiant heaters was based on a calculation involving the heat flux between the heaters and the wetted tank wall. The total heat input rate was based on additional calculations involving the power to the immersion heater and the time-averaged enthalpy change of the liquid flowing from the tank exit. The latter calculations required that the radiant heater calculation be normalized to obtain the total energy input to the liquid over the time to outflow. Justification for this normalization was based on no-flow and boiloff tests presented in reference 6, and the method is extended here to consider the immersion heater.

Heat Input Rate from Radiant Heaters

Each heater was considered to consist of three zones, each having a uniform temperature measured by a thermocouple in that zone.

The net radiant heat exchange was then calculated between each zone of a heater and the corresponding tank surface, assuming that both the heater and the wall were gray surfaces and the close spacing of the heater to the tank wall was analogous to concentric cylinders. The net heat exchange per unit tank area per unit time from each zone was computed from the equation

$$q = \sigma f_{T\text{-}H}\left(T_H^4 - T_T^4\right)$$

where σ is the Stefan-Boltzmann constant and

$$\frac{1}{f_{T\text{-}H}} = \frac{1}{\epsilon_T} + \frac{r_T}{r_H}\left(\frac{1}{\epsilon_H} - 1\right)$$

The symbols used in this report are defined in appendix A. Constant emissivities of 0.8 were assumed for both surfaces. The heat input rate from the heaters was then obtained from

$$\dot{Q}_H(x_s) = \int_0^{x_s} Kq \frac{dS}{dx}\, dx \tag{1}$$

where x_s is the height of liquid in the tank. Equation (1) will be normalized later as previously mentioned.

The time-averaged rate of heat input from the heaters was obtained by use of the expression

$$\bar{\dot{Q}}_H = \frac{1}{t_m}\int_0^{t_m}\int_0^{x_s(t)} Kq \frac{dS}{dx}\, dx\, dt \tag{2}$$

where t_m is the flow time required to empty the tank and $x_s(t)$ is obtained from the relation

$$V(L) - \dot{V}t = \int_0^{x_s(t)} \pi r^2(x)\, dx \tag{3}$$

where $\dot{V}$ is the average volumetric flow rate calculated from the slope of a straight-line curve fit of liquid volume history. The liquid volume history was obtained by observing the time at which the liquid surface passed the several temperature sensor locations.

Heat Input Rate from Immersion Heater

The total power delivered to all immersion heater elements at any given time ($\dot{Q}_N(t)$) as measured by $\sum_i \left[E^2(t)/R\right]_i$ was assumed to be entirely transferred to the liquid. As the liquid level passed below a given element, that element was disregarded in making the summation. The resistance of each element was measured prior to the run while the voltage supplied to each element was measured during each run.

The average heat input rate from the immersion heater during the flow run was obtained from the expression

$$\dot{\bar{Q}}_N = \frac{1}{t_m} \int_0^{t_m} \dot{Q}_N(t)\, dt \tag{4}$$

The location and power history of each element along with the previous relation of liquid level with time (eq. (3)) gave the total immersion heater power as a function of liquid height ($\dot{Q}_N(x_s)$).

Heating Rate of Liquid

The average heating rate of the liquid during a flow test was based on the time-averaged enthalpy increase in liquid flowing from the tank exit. The average increase in liquid temperature was first calculated from the expression

$$\overline{\Delta T} = \frac{1}{t_m} \int_0^{t_m} \Delta T(0,t)\, dt$$

where $\Delta T(0,t)$ is the measured increase in exit temperature at time t after start of flow and t_m is the time required to empty the tank. The average heating rate of the liquid was then obtained from the expression

$$\dot{\bar{Q}}_l = K\bar{\rho}\, \overline{c_p}\, \overline{\Delta T}\, \dot{V} \tag{5}$$

where $\bar{\rho}$ and $\overline{c_p}$ are the liquid density and specific heat at constant pressure evaluated at the average temperature $T_{in} + \overline{\Delta T}$ by using the National Bureau of Standards literature. The values of density and specific heat evaluated for each run are shown in table I.

The heating rate distribution in the liquid was considered as being provided by both immersion heater power and the heating rate from the radiant heaters. Because this assumption did not consider other heat inputs (such as radiant heat transfer from the dome, for instance), the radiant heater calcu-

lations were normalized to obtain equality among the time-averaged heating rates (eqs. (2), (4), and (5)), that is to obtain $\bar{\dot{Q}}_l = \bar{\dot{Q}}_N + \bar{\dot{Q}}_H$. The heating rate of the liquid is consequently given by the expression

$$\dot{Q}_l(x_s) = \dot{Q}_N(x_s) + \frac{\bar{\dot{Q}}_l - \bar{\dot{Q}}_N}{\bar{\dot{Q}}_H} [\dot{Q}_H(x_s)] \tag{6}$$

Specific values of the average heating rate from radiant heaters $\bar{\dot{Q}}_H$ and the heating error term $(\bar{\dot{Q}}_l - \bar{\dot{Q}}_N)/\bar{\dot{Q}}_H$ for each run are shown in table I.

Generalizing Parameters

Generalizing parameters were derived in reference 6 to make test results applicable to a wide range of operating conditions. The same parameters are derived herein, for completeness, along with an additional term to account for liquid heat sources. A system is assumed to consist of the liquid bounded by the tank walls and the liquid gas interface at anytime during flow. The assumptions are made that there is no heat transfer across the interface, that energy is time dependent and varies only in an axial direction, and that liquid properties are nonvariant and determined at a time-averaged temperature level. An energy balance of the system may be expressed in terms of the time rate of liquid enthalpy change, the rate at which enthalpy is being transported from the system and the total heating rate entering the system. In equation form, this is expressed as

$$K\bar{\rho}\ \overline{c_p}\ \frac{d}{dt} \int_{V(x_s)} \Delta T(x,t)dV + K\ \overline{c_p}\ \dot{w}\ \Delta T(0,t) = \dot{Q}_l(x_s) \tag{7}$$

where $\dot{w}$ is the weight flow rate and $V(x_s)$ is the volume of liquid in the tank at any given time.

A saturation heating rate $\dot{Q}_s$ is now defined as the energy required to heat the initial liquid content to saturation temperature in the same time required to empty the tank. This saturation heating rate can be expressed as

$$\dot{Q}_s = \frac{K\bar{\rho}\ \overline{c_p}\ V(L)\Delta T_s}{t_m} = K\ \overline{c_p}\ \dot{w}\ \Delta T_s \tag{8}$$

When equations (7) and (8) are combined, the energy equation then becomes

$$\frac{d}{d\tau} \int_{v(x_s)} \vartheta\left(\frac{x}{L},\tau\right)dv + \vartheta(0,\tau) = \frac{\dot{Q}_l(x_s)}{\dot{Q}_s} = \mathscr{Q}\left[\frac{\dot{Q}_l(x_s)}{\dot{Q}_l(L)}\right] \tag{9}$$

where

$$\left.\begin{aligned} \tau &= \frac{t}{t_m} & \vartheta &= \frac{\Delta T}{\Delta T_s} \\ v &= \frac{V(x)}{V(L)} = 1 - \tau & \dot{\mathcal{Q}} &= \frac{\dot{Q}_l(L)}{\dot{Q}_s} \end{aligned}\right\} \tag{10}$$

In this form the energy equation states that the nondimensional temperature history everywhere in the tank is a function of the nondimensional heating rate distribution $\dot{Q}_l(x_s)/\dot{Q}_l(L)$ and a heating parameter $\dot{\mathcal{Q}}$. The heating rate distribution, in some instances, originates from both heat transfer through the tank wall and from source heating in the liquid. When both terms exist, it is convenient to express the initial magnitude of liquid source heating in terms of the initial total heating $\dot{Q}_N(L)/\dot{Q}_l(L)$. Values of the initial total heating rate $\dot{Q}_l(L)$, the heating parameter $\dot{\mathcal{Q}}$, and the initial ratio of liquid source heating to total heating rate $\dot{Q}_N(L)/\dot{Q}_l(L)$ for each run are shown in table I.

RESULTS AND DISCUSSION

A series of tests was performed to document the use of an electrical immersion heater as a means of simulating nuclear heating of liquid hydrogen. The experimental data obtained from this series of tests are presented. Test results are used to show the effect of the presence of the inoperative immersion heater on the liquid behavior. Test results of simulated nuclear source heating are compared with results from nuclear heating tests (ref. 3). Results of two tests without source heating but having a relatively high ratio of bottom-to-wall heat flux (hereafter called high bottom heating) are also compared with results from the nuclear heating tests.

Experimental Data

The heat input rate calculated from the heaters as a function of liquid height is presented in figure 4 for the several tests. The data points show calculated values of heat input rate from the heaters obtained by using equation (1). The heat input rate distribution for run 1 (fig. 4(a)) was established by using a relatively low bottom radiant heater temperature and high wall heater temperature. This heat input configuration was selected to compare with a typical high wall heating configuration with no immersion heater installed (H - L configuration of ref. 6). The resultant average wall and bottom heat fluxes are given in table I. Relatively high bottom heating was used for run 2 (fig. 4(b)); this configuration was selected as representative of the type of heat input configuration which might be experienced in a nuclear rocket (see refs. 3 to 6). Run 3 (fig. 4(b)) is similar to run 2 in heat input configuration (within 10 percent) and is presented to illustrate the consistency of temperature history data. In the case of run 4, both the radiant heaters

and the immersion heater were used, and the respective heat input rates are shown in figures 4(c) and (d). Also shown are the heat input rates for another test using both sets of heaters, run 5. For the latter two runs, the magnitude of the heat input rates was about the same, but for run 5 the immersion heater elements were selectively turned off as the liquid level approached each element. This was done to observe if a measurable difference in results existed when the heaters were left on or turned off and will be discussed subsequently.

The temperature histories at several tank heights are presented in figure 5. In general, the temperature rise at any thermometer location increased after the start of flow. This increase in temperature rise with time shows an increase in temperature of the main bulk of liquid and, as the liquid level approaches a given location, an increase in temperature due to a stratified layer near the surface. The high wall heat configuration, run 1, shows a smooth increase in temperature rise at all locations (fig. 5(a)) with a trend toward an increasing temperature gradient with time throughout the height of liquid. For instance, 400 seconds after the start of flow the temperature rise was about 0.1° F at the tank outlet but at a height of 16.9 inches the temperature rise was about 0.3° F; at 24.7 inches, 0.5° F; etc. For the high bottom heat configurations (runs 2 and 3; figs. 5(b) and (c), respectively) or the simulated nuclear heating configurations (runs 4 and 5; figs. 5(d) and (e), respectively), a near constant temperature region existed to near the liquid surface. A comparison of figures 5(a) and (b), for instance, shows that the region of turbulently mixed (constant temperature) liquid is more extensive with high bottom heating than with high wall heating. These results are typical of high wall or high bottom heat configurations and have been previously observed (ref. 6).

It was seen, with the present experimental data, that the temperature at a thermometer location of 40.7 inches (initial surface level was about 44 in.) with high bottom heating had a tendency to increase. Then it levels for a short period (figs. 5(b) to (e)) shortly after the start of flow and before the liquid surface dropped a significant amount. A similar tendency was not observed with high wall heating (run 1, fig. 5(a)). A review of previous wall and bottom heating data (ref. 6) showed that this phenomenon was consistent. A discussion of the transient development of a temperature gradient near the surface is presented in appendix B along with additional temperature data near the surface during the first portion of test run 4.

Effect of Immersion Heater Installation on Liquid Behavior

Perhaps the most profound effect of the presence of the immersion heater on liquid behavior was expected at the liquid gas interface when the liquid surface passed each element. A disruption of the placid surface did occur during the flow of the liquid surface past the elements which could be seen from viewing the liquid with a television system. As the liquid surface drops past the element, the surface is disrupted into small waves which disappear after a few seconds. This disturbance was observed to occur each time the surface passed a visible heater element. The immersion heater elements appear to have perturbed the liquid surface during outflow; however, the significant effect of any change in liquid behavior should appear as a change in tank pressure or in

the exit temperature history. Evaporation and/or condensation was anticipated due to the additional wetted surface of each heater element above that of the tank wall alone. However, the liquid surface passing each element did not result in a noticeable change in tank pressure.

A comparison of generalized test results with and without the immersion heater installed is presented in figure 6. Both the generalized heating rate distribution (fig. 6(a)) and the exit temperature history (fig. 6(b)) are shown for run 1 obtained with the immersion heater installed and for a similar run (H - L configuration from ref. 6) without the heater installed. A comparison of heating rate distributions indicates that the two cases were obtained with nearly the same generalized heat input. A comparison of the resultant generalized exit temperature histories shows a general consistency in shape between the two curves, which indicates the liquid behavior was not overly influenced by the presence of the immersion heater. The temperature history of run 1 ($\dot{\mathcal{Q}} = 0.444$) shows a trend toward a higher temperature, as expected, than that of the run (ref. 6) without the heater ($\dot{\mathcal{Q}} = 0.429$). There was a noticeable increase in time during which the exit thermometer indicated saturation temperature rise with the heater installed (fig. 6). This trend existed at other thermometer locations, even at locations above the height of the heater (see fig. 5, for instance). It is doubtful, therefore, that this difference resulted from the heater installation.

Electrically Simulated Nuclear Heating

The generalized test results with electrically simulated nuclear heating are presented in figure 7. The results obtained from test runs 4 and 5 are compared with the results of a nuclear heating test having a similar value of heating parameter (run 18.100, ref. 3). Two heating rate distribution curves are shown in figure 7(a) for each run. The top curve depicts the total heating rate distribution both from heat transferred to the liquid from the tank walls and from heat sources in the liquid; the latter is shown separately by the bottom curve. The total heating rate of the liquid for run 4 (fig. 7(a)) closely matched that of the nuclear heating run although the amount of liquid source heating for run 4 was considerably less for two reasons: (1) the heating load (power per unit volume) applied to each element was about 40 percent less, and (2) the immersion heater extended up to about half of the initial liquid height. The results obtained from run 4 (to be discussed later) made it unnecessary to conduct further tests with increased heating loads.

The low total heating rate of the liquid for run 5 (fig. 7(a)) at low liquid heights resulted from turning off the power to successive immersion heater elements before the liquid level came within several inches of any particular element. This was done in an effort to avoid perturbing the stratified layer near the liquid surface by power generation. The initial liquid source heating rate was about the same for both tests (runs 4 and 5), and consequently, the difference in liquid height for any given liquid source heating rate indicates the approximate height of liquid above an element when its power was turned off.

The generalized exit temperature histories for the two simulated nuclear heating runs are shown in figure 7(b) and compared with the results of the nuclear heating test. The results of all three tests appear, in general, to be about the same during the early portion of the tests. In the last quarter of the flow period, a more significant difference appears. The exit temperatures of the simulated nuclear tests show a tendency toward a more rapid increase in temperature. With nearly equal total heating rate distributions between run 4 and the nuclear data (see fig. 7(a)), consistent temperature histories were anticipated as a function of heating parameter. That is, the higher the heating parameter, the greater the temperature rise at any given time from start of flow (see ref. 6, for instance). Although the heating parameter for the nuclear data ($\dot{\mathcal{Q}} = 0.457$) was slightly higher than the present test run 4 ($\dot{\mathcal{Q}} = 0.434$), the early history indicates an exit temperature rise which is less by a small amount. This trend indicates more heat has been stored in the stratified layer during the nuclear run. A comparison of the exit temperature histories near the end of the tests shows the previously stored heat in the nuclear case resulted in an increase in temperature rise greater than those of the present test.

A comparison of the results of run 5 and the nuclear data shows similar trends as the previous comparison. In this instance, the difference in temperature histories occurred with about the same heating parameter but with different generalized heat input distributions. Apparently the heating rate at low liquid height for run 5, being less than the nuclear data, resulted in lower exit temperatures near the end of the run.

The previous comparisons show that, in general, the nuclear heating could be simulated by the use of an electrical immersion heater. The trend toward a more completely mixed liquid with the immersion heater was taken to indicate no further purpose would be fulfilled by applying a higher heating load to simulate more closely the nuclear liquid source heating. An attempt to reduce the indicated mixing effect by turning off the power to each element before the surface passed the element resulted in a change of heating rate distribution. Another feasible simulation of the total nuclear heating rate distribution was indicated in reference 6 by the use of bottom heating.

Comparison of Bottom and Nuclear Heating

Two tests were performed (runs 2 and 3) in which the bottom and wall heat flux were established to approximate the heating rate distribution obtained with the nuclear heating data of reference 3. The results of these tests are compared with results of a nuclear test in figure 8. A comparison of the generalized heating rate distribution (fig. 8(a)) shows that the total heat rate distribution is about the same for all tests although in the nuclear case, about 70 percent of the heat input was deposited directly into the liquid. The initial total heating rate of the nuclear data was over six times greater than that of either of the present tests (see fig. 8(a)). A comparison of the generalized exit temperature histories (fig. 8(b)) shows that the results of test run 2 and those of the nuclear test were almost identical. These three tests

also had similar heating parameters despite the factor of 6 variation in the total initial heating rates. Test run 3 yielded a generalized exit temperature history consistent with its 3-percent-lower heating parameter.

A comparison of figures 7 and 8 indicates that bottom heating tests more closely simulated the nuclear heating test results than the electrical immersion heater tests. Apparently the liquid behavior associated with the bottom heating tests resulted in a turbulent flow field similar to that with nuclear heating. The high degree of attenuation associated with nuclear radiation in both liquid hydrogen and the tank material (along with the uniform nature of the nuclear heat deposition) appears to result in liquid behavior similar to that experienced with convective heat flow from the tank bottom.

The major contribution to turbulence is perhaps more from bottom heating than the liquid heat sources in nuclear heating. The liquid behavior near the surface during the early period of flow (see discussion in appendix B) suggested that high bottom heating consistently influences the establishment of the depth of the stratified layer. This condition also existed with about the same heat flux on both wall and bottom (H - H configuration of ref. 6). It seems possible, therefore, that the nuclear heating of the tank material, as opposed to the liquid source heating, may have had an overriding influence on the establishment of flow behavior.

SUMMARY OF RESULTS

The following results were obtained from an experimental study to simulate nuclear heating of liquid hydrogen in a tank by means of an electrical immersion heater and radiant heaters.

1. The use of an electric immersion heater to simulate nuclear heat sources in the liquid tended to result in a more completely mixed state of liquid than with nuclear heating.

2. Simulating the generalized heating rate distribution of nuclear heating by means of radiant heaters gave nearly identical generalized exit temperature histories with similar heating parameters despite unsimilar operating conditions.

3. The presence of the 1/4- by 1-inch grid network of the immersion heater appeared to perturb the liquid surface while dropping past the heater elements but without affecting the exit temperature history.

4. High bottom (or liquid source) heating was observed to consistently result in a disturbance of liquid near the surface during the transient development of a temperature gradient.

Lewis Research Center,
National Aeronautics and Space Administration,
Cleveland, Ohio, December 13, 1965.

APPENDIX A

SYMBOLS

c_p	specific heat of liquid at constant pressure, Btu/(lb)($^\circ$R)
E	voltage to heater
f	gray-body shape factor
K	conversion factor, W/(Btu/sec)
L	initial liquid height in tank, ft
P_T	tank pressure, psia
$\dot{Q}$	heating rate, W
$\dot{\mathcal{Q}}$	ratio of heating rates, heating parameter
q	heat flux, Btu/(sec)(ft^2)
R	heater element resistance, ohms
r	radius, ft
S	tank surface area, ft^2
T	temperature, $^\circ$R
t	time from start of flow, sec
V	tank volume, ft^3
$\dot{V}$	volumetric flow rate, ft^3/sec
v	ratio of volumes
$\dot{w}$	weight flow rate, lb/sec
x	height from tank bottom, ft
ϵ	emmissivity
ϑ	ratio of temperature rises
ρ	density, lb/ft^3
σ	Stefan-Boltzmann constant, Btu/(sec)(ft^2)($^\circ$F^4)

τ ratio of times

Subscripts:

b bottom

H heater, radiant

i unit

in initial

l liquid

m maximum

N liquid source

s saturation, surface

T tank

w wall

Superscript:

— time-averaged value

APPENDIX B

TRANSIENT DEVELOPMENT OF TEMPERATURE GRADIENT

In the discussion of figure 5 it was observed that the temperature indicated by the carbon-resistor thermometers near the initial surface level sometimes had a tendency to increase and then level off for a brief period shortly after the start of flow. This tendency was observed only with heating rate distributions having high bottom heating rates. This phenomenon was explored more fully during run 4 by recording each thermometer output at 0.054-second intervals from the time the tank was closed until several seconds after the start of flow. Twenty-five consecutive measurements of each thermometer were averaged to reduce the effect of 60 cycle noise in the signals resulting in averaged data points 1.35 seconds apart.

The resultant temperature histories of several thermometers are presented in figure 9. Also shown is the saturation temperature history. Thermometers 1 through 13 are spaced at 1/4-inch axial increments; 14 is 4 inches below 13, and 15 is 4 inches below 14 (ref. 6). Thermometer 1 is 43.69 inches above the tank bottom. The temperatures measured at thermometer 15 are typical of temperatures below this location. The tank was closed 20 seconds before the start of flow; pressurization started 5 seconds after the tank was closed. Closing the tank caused the tank to self pressurize until the addition of pressurant. Pressurization of the tank resulted in an increase in liquid temperature due, probably, to isentropic compression of liquid. A temperature gradient also developed in the top 2 or 3 inches of liquid during the time interval from pressurization to the start of flow. The initial liquid level (as indicated by saturation temperature after pressurization) appears to be slightly above the position of thermometer 1. After the start of flow, the general trend toward increasing temperature with time at any given location is the result of heat addition and a decrease in liquid level with outflow but disturbances seem to appear in the upper regions of liquid (above thermometer 14) causing variations in indicated temperature histories at certain locations.

The first disturbance occurred about 2 seconds after the start of flow. The change in temperature level was experienced almost simultaneously throughout the upper region and probably resulted from a slight adjustment of liquid volume in the tank upon opening the shutoff valve and filling the outlet piping to the throttle valve. The volume adjustment would be observable in the upper region by changes in temperature level because of the existing temperature gradient. No effect of volume adjustment is noticeable without the gradient. A second disturbance occurred about 12 seconds after the start of flow. This change in temperature level was again experienced simultaneously but only near the surface (thermometers 3 to 7).

A third disturbance about 15 seconds after the start of flow appeared as temperature-level changes of longer duration (until about 40 sec after start of flow) and progressed downward with time. The downward progression is observed by the initial temperature level change occurring at lower locations with increased time. The progression continues for a depth of several thermometer

locations in about the same interval of time required for the liquid surface to drop the 1/4-inch distance between two thermometers.

It is probable that the third disturbance resulted from a quantity of warm liquid having traveled toward the surface (probably along the tank wall), turning radially inward near the surface, meeting with other warm liquid at the center, and being forced downward before dissipating. This phenomenon was also observed in the two-dimensional tank tests of reference 2. Schlieren photographs of the early history of flow tests (in ref. 2) showed a downward flow of warm liquid with either wall heating or a combination of wall and bottom (or nonuniform source) heating. However, in the liquid hydrogen experiments (present data and ref. 6) the results of this downward progression were observed only with high bottom (or nonuniform source) heating. The transient development of a quasi-steady-state temperature gradient in liquid hydrogen is thus seen to be dependent on the heating rate distribution into the liquid. Wall heating of liquid hydrogen appears to contribute in a smooth manner to the development of temperature gradients which may extend over the major depth of liquid (see fig. 5(a), for instance). Bottom heating, on the other hand, contributes to a generally more turbulent flow of fluid which disturbs the wall heating contribution to the temperature gradient within a short time period (about 15 sec in the example shown) and results in a thinner stratified layer above a region of turbulently mixed liquid.

REFERENCES

1. Vliet, G. C.: Stratified Layer Flow Model: A Numerical Approach to Temperature Stratification in Liquids Contained in Heated Vessels. Aerospace Sci. Lab., Lockheed Missiles and Space Co., Nov. 1964.

2. Anderson, Bernhard H.; and Kolar, Michael J.: Experimental Investigation of the Behavior of a Confined Fluid Subjected to Nonuniform Source and Wall Heating. NASA TN D-2079, 1963.

3. Hehs, W. A.; McCauley, B. O.; Miller, G. E.; and Wheeler, D. M.: Nuclear Radiation Heating in Liquid Hydrogen. NASA CR-54078, 1964.

4. Anderson, B. H.; Huntley, S. C.; and Connolley, D. J.: Propellant Heating Studies with Wall and Nuclear Heating. Paper No. 64-WA/AV-8, ASME, Nov.-Dec. 1964.

5. Anderson, Bernhard H.; and Danilowicz, Ronald L.: Analytical and Experimental Study of Nuclear Heating of Liquid Hydrogen. NASA TN D-2934, 1965.

6. Huntley, S. C.; Gauntner, J. W.; and Anderson, B. H.: Wall and Bottom Heating of Liquid Hydrogen in a Propellant Tank. NASA TN D-3256, 1966.

TABLE I. - TEST CONDITIONS

Run	1	2	3	4	5
Type of heating	Radiant			Radiant and immersion	
Average heat flux, Btu/(ft^2)(sec)					
Wall, q_w	0.0082	0.0035	0.0031	0.0040	0.0040
Bottom, q_b	0.0003	0.0083	0.0071	0.0073	0.0071
Initial liquid height, L, in.	43.94	44.20	43.49	43.79	42.31
Initial temperatures, T_{in}, ^{o}R	38.25	38.25	38.30	38.20	38.44
Tank pressure, P_T, psia	33.78	34.00	34.22	34.76	34.67
Saturation temperature rise, ΔT_s, ^{o}F	3.95	4.00	4.00	4.22	3.96
Average flow rate, $\dot{w}$, lb/sec	0.0404	0.0405	0.0368	0.0407	0.0401
Average density, $\overline{\rho}$, lb/ft^3	4.310	4.316	4.297	4.303	4.296
Average specific heat, $\overline{c_p}$, Btu/(lb)(^{o}R)	2.48	2.54	2.54	2.57	2.58
Average heating rate from heaters, $\dot{\overline{Q}}_H$, W	63.15	59.10	52.34	60.93	64.94
Heating error term, $(\dot{\overline{Q}}_l - \dot{\overline{Q}}_N)/\dot{\overline{Q}}_H$	1.277	1.654	1.586	1.486	1.386
Initial total heating rate of liquid, $Q_l(L)$, W	184	141	121	202	200
Ratio of source to total heating, $\dot{Q}_N(L)/Q_l(L)$	---	---	---	0.308	0.316
Heating parameter, $\mathcal{Q}$	0.444	0.325	0.306	0.434	0.462

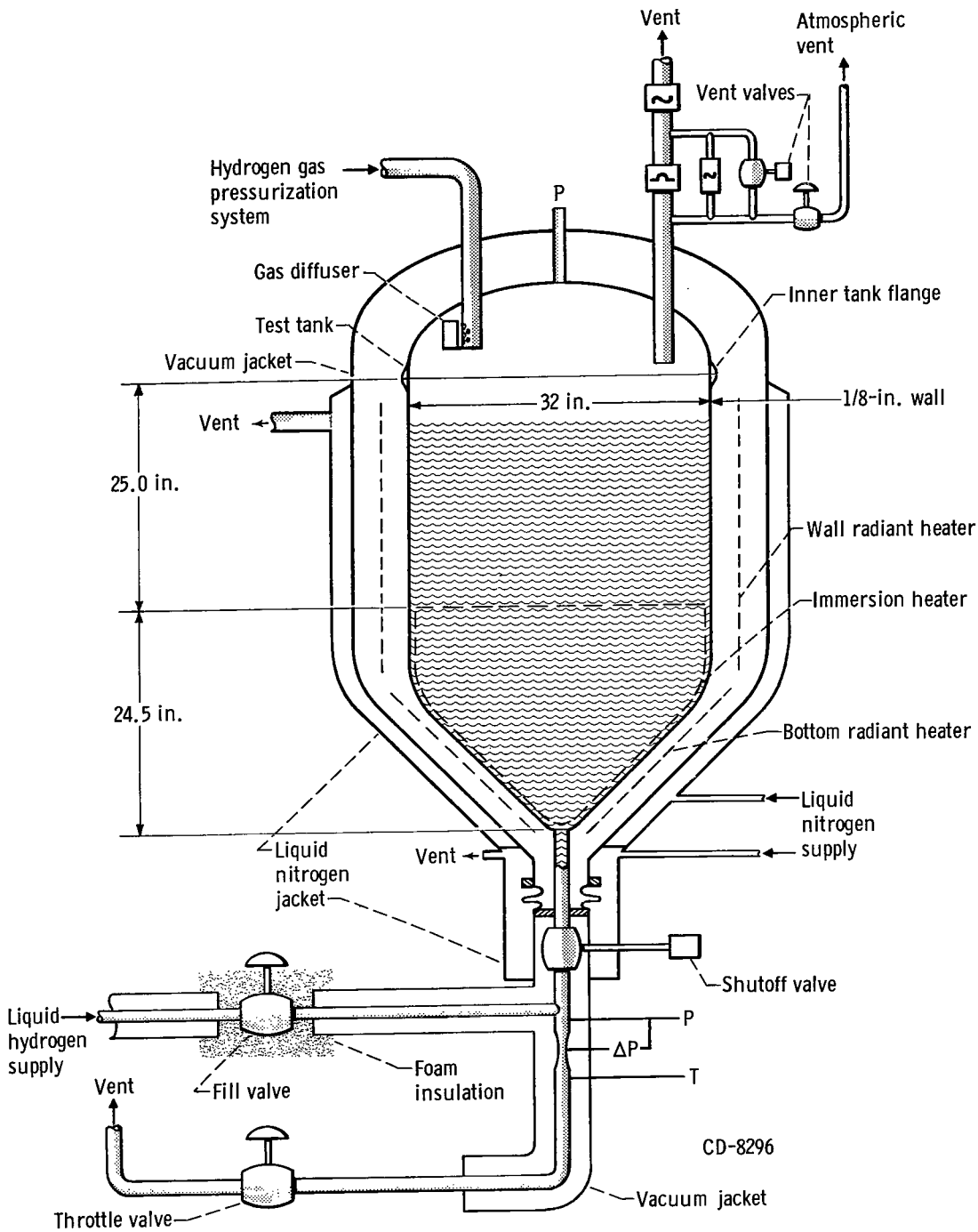

Figure 1. - Schematic of test apparatus.

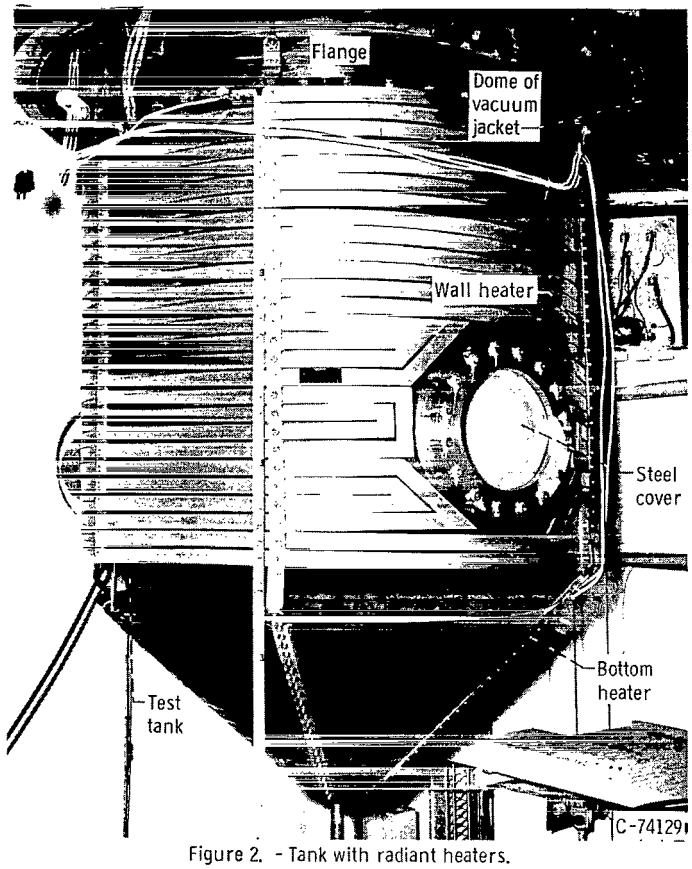

Figure 2. - Tank with radiant heaters.

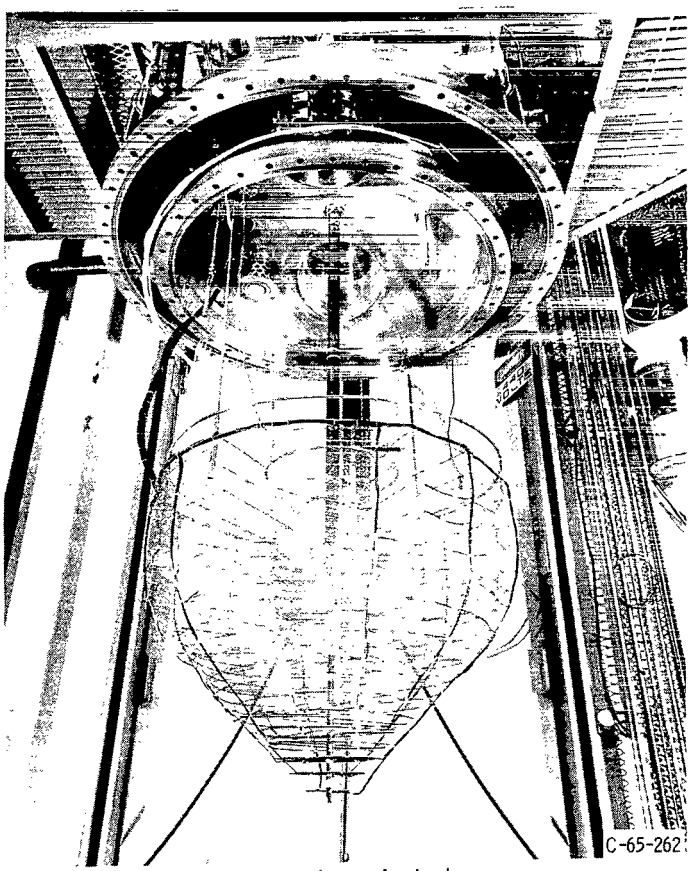

Figure 3. - Immersion heater.

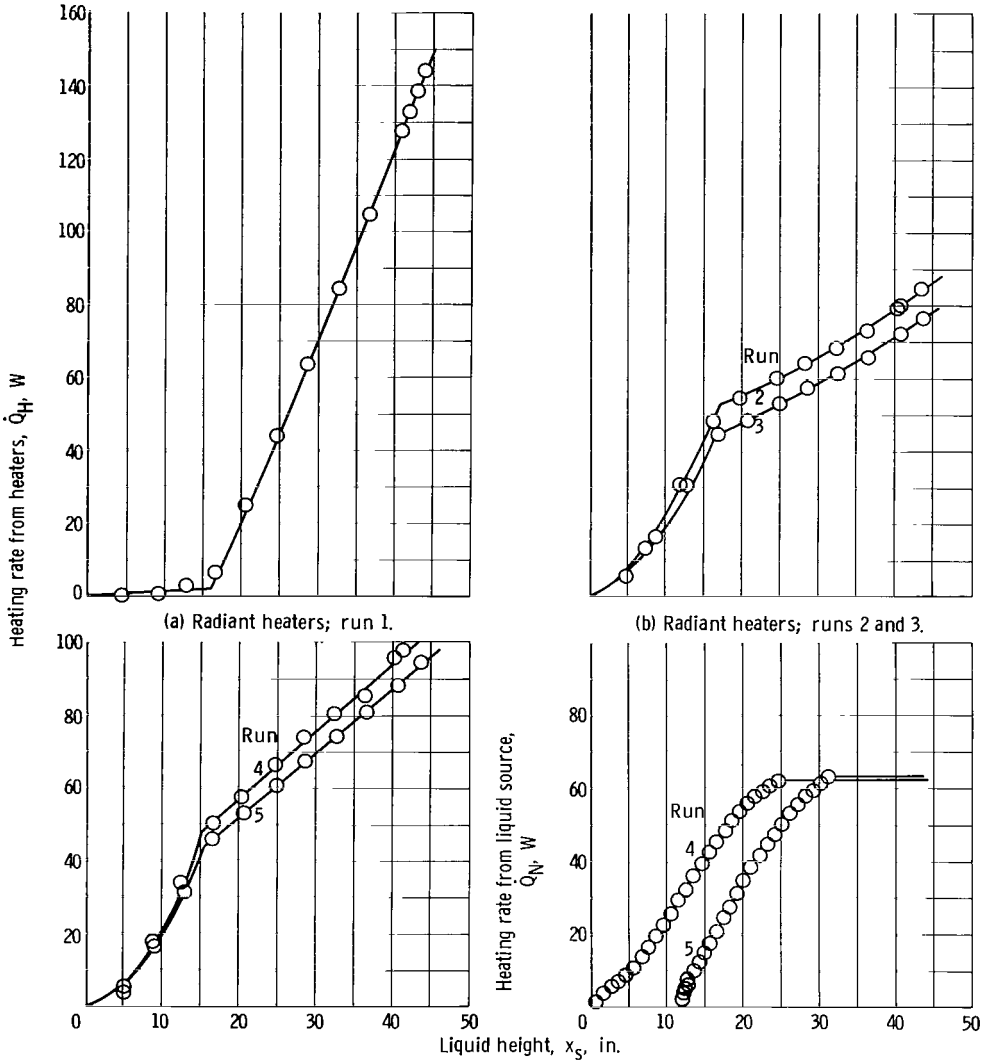

Figure 4. - Heating rate distribution from heaters.

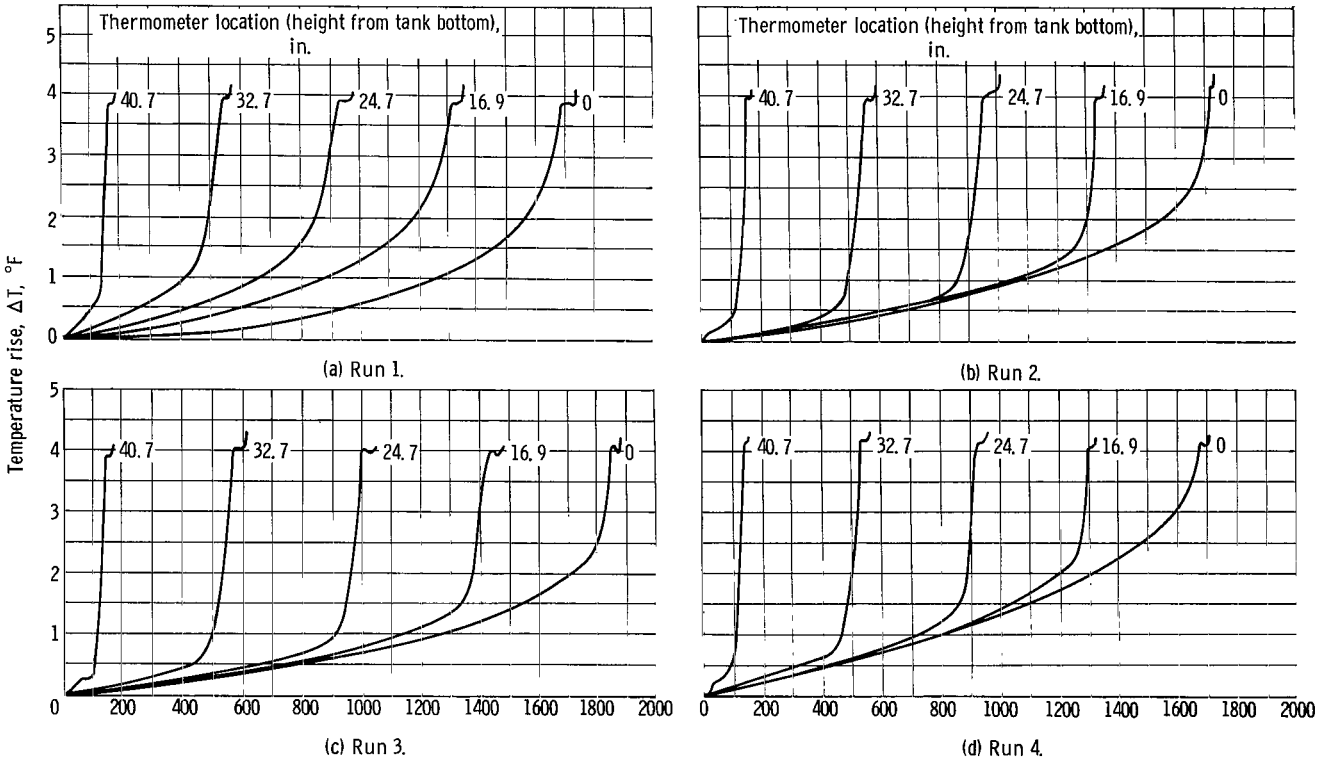

(a) Run 1.

(b) Run 2.

(c) Run 3.

(d) Run 4.

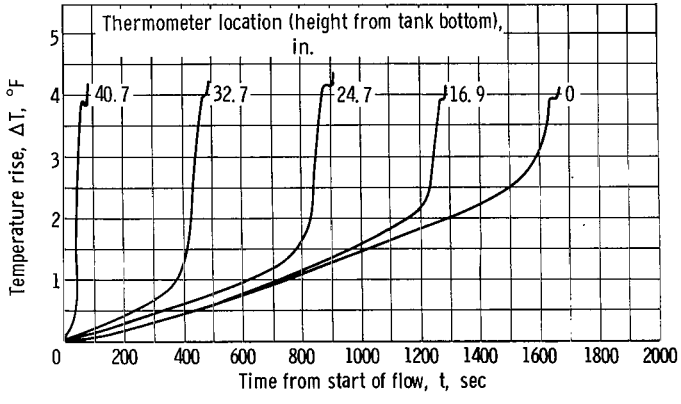

(e) Run 5.

Figure 5. - Temperature histories.

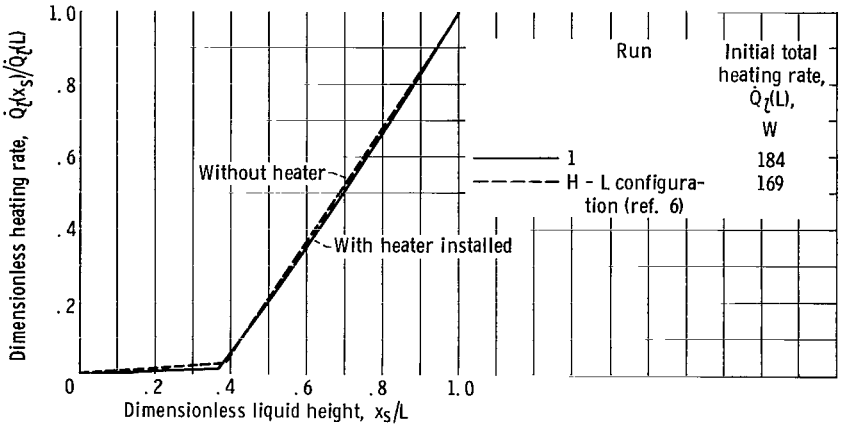

(a) Heating rate distribution.

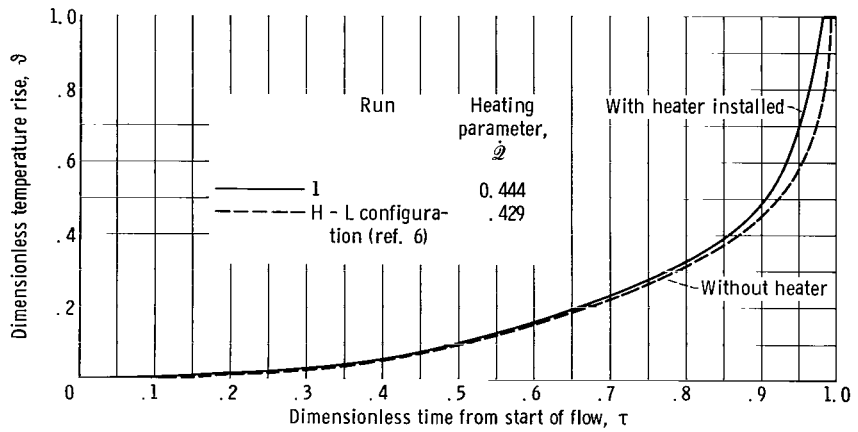

(b) Exit temperature history.

Figure 6. - Comparison of generalized test results with and without immersion heater installed.

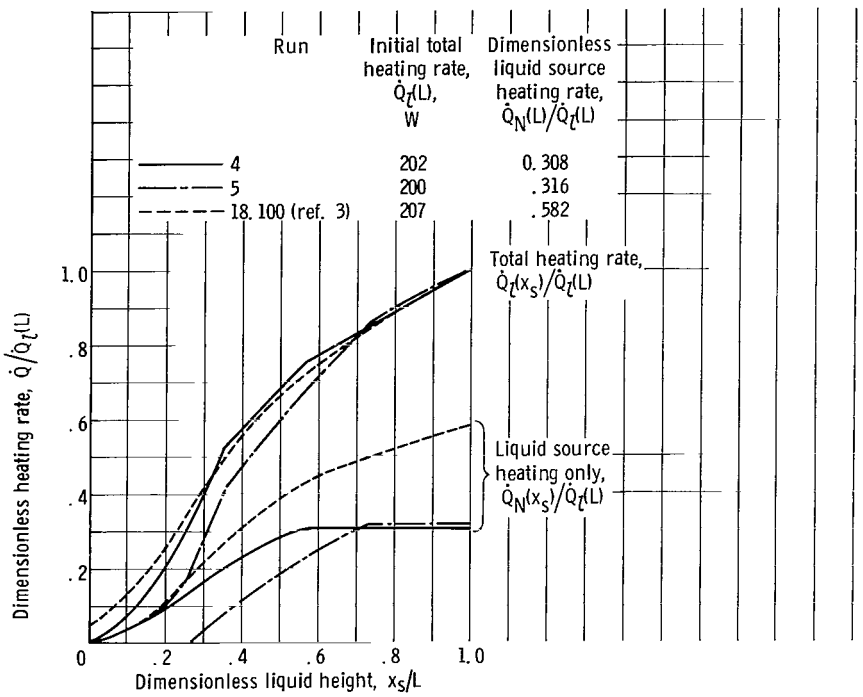

(a) Heating rate distribution.

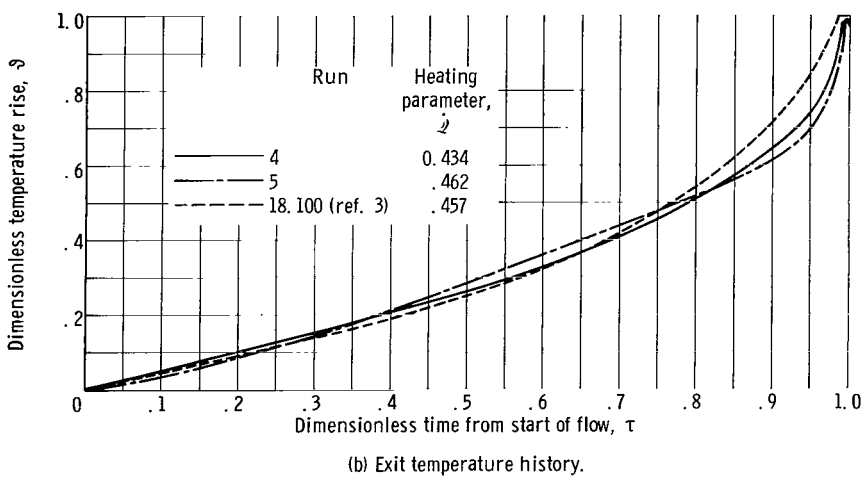

(b) Exit temperature history.

Figure 7. - Comparison of generalized test results with liquid source heating.

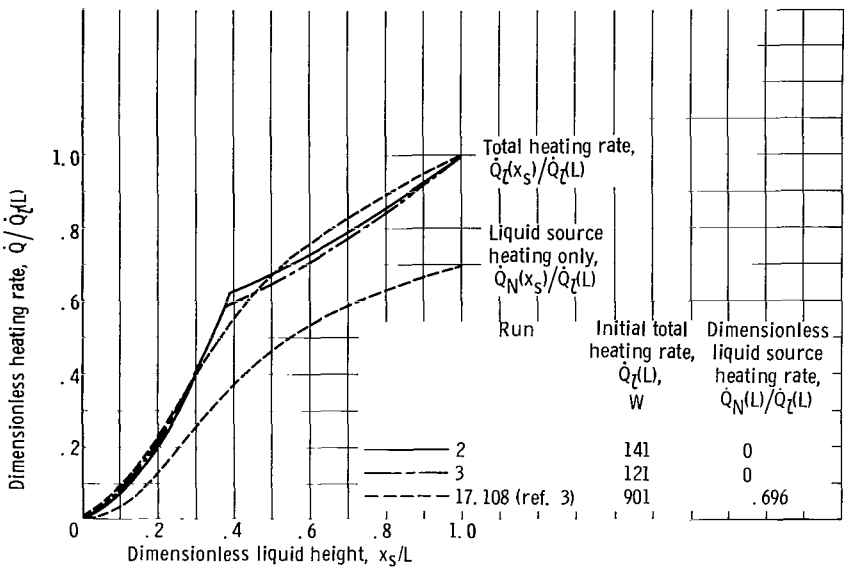

(a) Heating rate distribution.

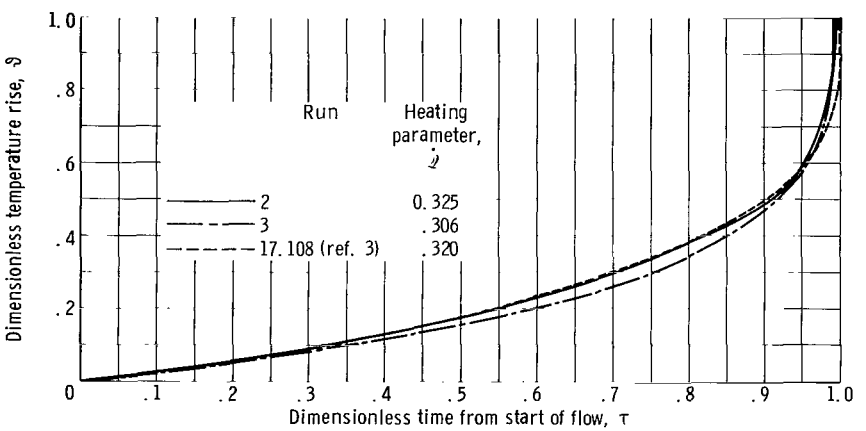

(b) Exit temperature history.

Figure 8. - Comparison of bottom and nuclear heating data.

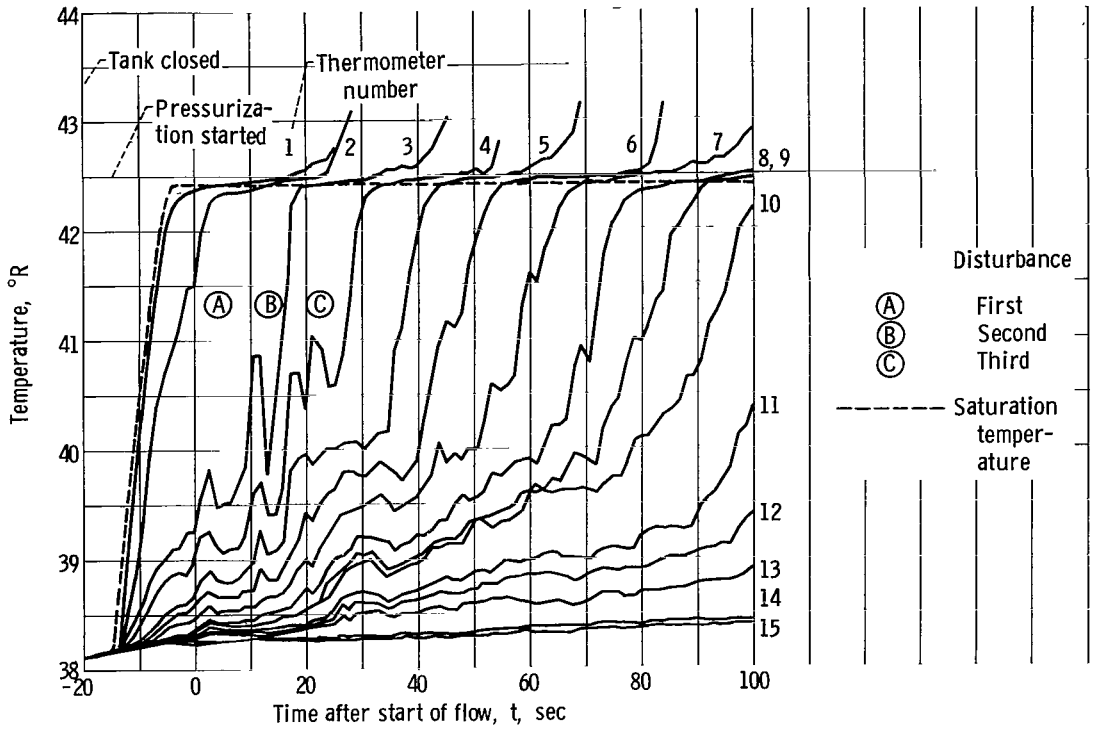

Figure 9. - Temperature history during transient development of temperature gradient.

"The aeronautical and space activities of the United States shall be conducted so as to contribute . . . to the expansion of human knowledge of phenomena in the atmosphere and space. The Administration shall provide for the widest practicable and appropriate dissemination of information concerning its activities and the results thereof."

—NATIONAL AERONAUTICS AND SPACE ACT OF 1958

NASA SCIENTIFIC AND TECHNICAL PUBLICATIONS

TECHNICAL REPORTS: Scientific and technical information considered important, complete, and a lasting contribution to existing knowledge.

TECHNICAL NOTES: Information less broad in scope but nevertheless of importance as a contribution to existing knowledge.

TECHNICAL MEMORANDUMS: Information receiving limited distribution because of preliminary data, security classification, or other reasons.

CONTRACTOR REPORTS: Technical information generated in connection with a NASA contract or grant and released under NASA auspices.

TECHNICAL TRANSLATIONS: Information published in a foreign language considered to merit NASA distribution in English.

TECHNICAL REPRINTS: Information derived from NASA activities and initially published in the form of journal articles.

SPECIAL PUBLICATIONS: Information derived from or of value to NASA activities but not necessarily reporting the results of individual NASA-programmed scientific efforts. Publications include conference proceedings, monographs, data compilations, handbooks, sourcebooks, and special bibliographies.

Details on the availability of these publications may be obtained from:

SCIENTIFIC AND TECHNICAL INFORMATION DIVISION

NATIONAL AERONAUTICS AND SPACE ADMINISTRATION

Washington, D.C. 20546